

Epicardial Suction: A New Approach to Mechanical Testing of the Passive Ventricular Wall

R. J. Okamoto

Department of Mechanical Engineering,
Washington University,
St. Louis, MO 63130

M. J. Moulton

Division of Cardiothoracic Surgery,
Washington University,
St. Louis, MO 63130

S. J. Peterson

Department of Mechanical Engineering,
Washington University,
St. Louis, MO 63130

D. Li

Mallinckrodt Institute of Radiology,
Washington University,
St. Louis, MO 63130

M. K. Pasque

Division of Cardiothoracic Surgery,
Washington University,
St. Louis, MO 63130

J. M. Guccione

Department of Mechanical Engineering,
Division of Cardiothoracic Surgery,
Washington University,
St. Louis, MO 63130

The lack of an appropriate three-dimensional constitutive relation for stress in passive ventricular myocardium currently limits the utility of existing mathematical models for experimental and clinical applications. Previous experiments used to estimate parameters in three-dimensional constitutive relations, such as biaxial testing of excised myocardial sheets or passive inflation of the isolated arrested heart, have not included significant transverse shear deformation or in-plane compression. Therefore, a new approach has been developed in which suction is applied locally to the ventricular epicardium to introduce a complex deformation in the region of interest, with transmural variations in the magnitude and sign of nearly all six strain components. The resulting deformation is measured throughout the region of interest using magnetic resonance tagging. A nonlinear, three-dimensional, finite element model is used to predict these measurements at several suction pressures. Parameters defining the material properties of this model are optimized by comparing the measured and predicted myocardial deformations. We used this technique to estimate material parameters of the intact passive canine left ventricular free wall using an exponential, transversely isotropic constitutive relation. We tested two possible models of the heart wall: first, that it was homogeneous myocardium, and second, that the myocardium was covered with a thin epicardium with different material properties. For both models, in agreement with previous studies, we found that myocardium was nonlinear and anisotropic with greater stiffness in the fiber direction. We obtained closer agreement to previously published strain data from passive filling when the ventricular wall was modeled as having a separate, isotropic epicardium. These results suggest that epicardium may play a significant role in passive ventricular mechanics. [S0148-0731(00)00305-8]

Keywords: Constitutive Relations, Finite Elements, Stress Analysis

Introduction

Mathematical models are needed to provide a sound basis for interpreting the nonhomogeneous changes in cardiac mechanical function that occur in regional pathological disorders, such as ischemic heart disease [1], in terms of changes in the local properties of the heart muscle. Existing models incorporate detailed descriptions of the three-dimensional ventricular topology, the internal fibrous architecture of the ventricular walls, and information about the ventricular pressures [2,3]. The ability of these models to predict the mechanical behavior of the heart accurately depends, however, on an accurate description of the intrinsic material properties of the ventricular wall.

In vitro biaxial testing protocols performed on isolated sheets of ventricular muscle suggest that passive myocardium is nonlinear, anisotropic, nearly elastic, and possibly regionally heterogeneous [4–7]. These sheets are cut so that the muscle-fiber axis lies in the plane of the section and the fiber orientation is relatively uniform through the thickness of the sample, but the extent to which these results reflect the material properties of intact myocardium remains uncertain. In order to make these tests, it is necessary to disrupt the structural integrity of the myocardium, and the specimen may be further damaged by contracture induced by ischemia or by calcium released from cells injured during the cutting process [6]. Moreover, it is not possible to reproduce either the compressive loading or the shear loading that occurs *in vivo* using this testing method.

Passive material properties of intact ventricular wall have been estimated using the conservation laws of continuum mechanics [8,9], but only under the assumption of material homogeneity. However, neither type of experiment provides information on transverse shearing properties in the circumferential–radial and longitudinal–radial planes because transverse shear strains are negligible in the isolated, arrested heart undergoing passive inflation [10]. These material properties are needed not only for mathematical models of passive ventricular filling. They are also very important for models of the beating heart in which systolic contraction is modeled by defining the stress tensor as the sum of the passive three-dimensional stress and an active fiber-directed stress [11]. Significant circumferential–radial and longitudinal–radial transverse shear strains during systole were reported by Waldman and co-workers [12].

Therefore, the purpose of this study was to use a new approach, termed epicardial suction, to quantify the material properties of intact canine left ventricular wall, especially those related to transverse shear.

Methods

An overview of the approach is shown in Fig. 1. Epicardial suction is a new technique that produces local deformation in an intact heart. In contrast to experiments using beating hearts or passive inflation of isolated, arrested hearts, the deformation occurs primarily in the region of the left ventricle (LV) where the suction cup is placed. The suction pressure is varied periodically, producing a repeatable pattern of deformation. The deformation is measured using a magnetic resonance imaging (MRI) technique known as MR tagging. This technique allows noninvasive measurement of displacements at numerous locations in the image

Contributed by the Bioengineering Division for publication in the JOURNAL OF BIOMECHANICAL ENGINEERING. Manuscript received by the Bioengineering Division April 27, 1999; revised manuscript received May 30, 2000. Associate Technical Editor: J. D. Humphrey.

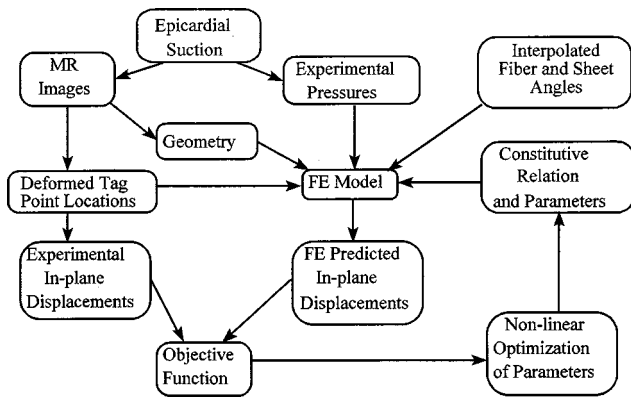


Fig. 1 Overview of the method for optimizing material properties using the epicardial suction. Epicardial suction is applied to a site on the LV. Geometry MR images are used to create an FE model that matches the experimental geometry and location of the suction cup. Measured pressures are used to define the loading for the FE model. Deformed and undeformed tag point locations are used to determine displacements. FE predicted displacements are interpolated from the FE model solution using the deformed tag point locations. At each iteration, the optimization algorithm solves the forward FE problem and calculates the sum of squares of the difference between predicted and measured displacements at all data points. Material parameters in the constitutive relation used in the FE model are adjusted iteratively to minimize the sum of squares objective function.

plane. By obtaining multiple sets of images in two orthogonal planes, the in-plane components of the three-dimensional displacements are determined. Additional MR images are acquired to document the position of the cup on the epicardial surface and create geometry for a finite element (FE) model of the heart. The FE model geometry is combined with measured epicardial suction pressures and previously published fiber angle data [2] to create an FE model of the experiment. The FE model solution is used to predict displacements in the plane of the image at the locations where the displacements were measured experimentally. At each iteration, the optimization algorithm solves the FE model and calculates the sum of squares of the difference between the FE predicted and experimental displacements. The algorithm adjusts the values of material parameters in a chosen constitutive relation to minimize the objective function. The method is not restricted to a particular form of constitutive relation; however, in this paper we use an exponential, transversely isotropic form.

Animal Preparation. Adult mongrel dogs ($n=8$, mean weight 22 kg) were anesthetized with pentobarbital (30 mg/kg IV), and mechanically ventilated. A median sternotomy was used to expose the heart. After administration of intravenous heparin (3 mg/kg), the aorta and great vessels were ligated, and the heart was arrested by injecting 1000 ml of a hypothermic (4°C) cardioplegic solution (Plegisol, Abbott Laboratories, Abbott Park, IL) into the root of the ascending aorta. The heart was excised and rinsed, and the atria were trimmed. The dogs received humane care in compliance with the principles of laboratory care formulated by the National Society for Medical Research and the most recent NIH guidelines. After cutting the chordae tendineae and removing the mitral valve, an acrylic support ring was sutured to the mitral annulus. The ring was attached so that it did not deform the base of the LV.

Creation of Epicardial Suction. A schematic drawing of the experimental setup is shown in Fig. 2. A suction cup with a square orifice approximately 2.5×2.5 cm (Fig. 3) was positioned on the lateral free wall of the LV. The suction cup was attached to the epicardium by vacuum pressure (12 kPa) applied continuously in

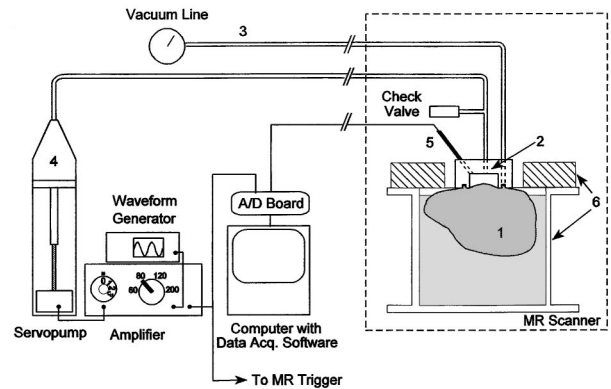


Fig. 2 Experiment setup, showing: (1) isolated arrested heart in cold saline solution; (2) suction cup; (3) vacuum applied continuously in narrow channel surrounding orifice; (4) servopump; (5) suction pressure measurement; (6) holding fixture and MR orbit coil (cross-hatched). A clamp holding the suction cup in position has been omitted for clarity.

the narrow channel surrounding the cup. The square suction orifice allowed the boundaries of the cup to be easily represented in our FE model. The suction cup was then attached to the holding fixture and the suction cup and heart were then lowered into the acrylic cylinder filled with a mixture of cold saline and cardioplegic solution. We used this hypothermic solution to prevent ischemic damage to the heart for up to four hours after arrest [13]. The suction cup was positioned so that the LV long axis was approximately horizontal.

Cyclical suction at a frequency of 2 Hz was created in the orifice by a positive displacement servopump (SPS3891, Vivitro Systems, Victoria, BC) driven by a sinusoidal signal from a waveform generator (Part WG5891, Vivitro Systems) and amplifier. The cyclical suction periodically reduced the suction pressure to zero, preventing the myocardium from creeping into the suction cup. A check valve opened at approximately 0.4 kPa gage pressure to prevent large positive pressures in the suction orifice that could detach the suction cup from the epicardium. The suction pressure was measured using a micromanometer catheter (Millar 5F Mikro-Tip, Millar Instruments, Houston, TX) introduced into the side of the cup.

MRI Protocol. Initial MR images were used to verify that the suction cup had been centered between the anterior and posterior papillary muscles of the LV for the lateral free-wall site. The amount of deformation during the application of epicardial suction was measured with a grid of magnetically “tagged” planes using a technique known as double Delays Alternating with Nutations for Tailored Excitation (DANTE) described by Mosher and Smith

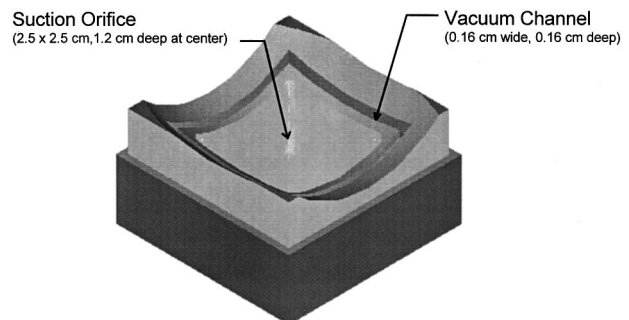


Fig. 3 Suction cup with concave surface of nonuniform curvature. The surface was contoured to approximately match the radii of curvature of the lateral free wall of the canine LV.

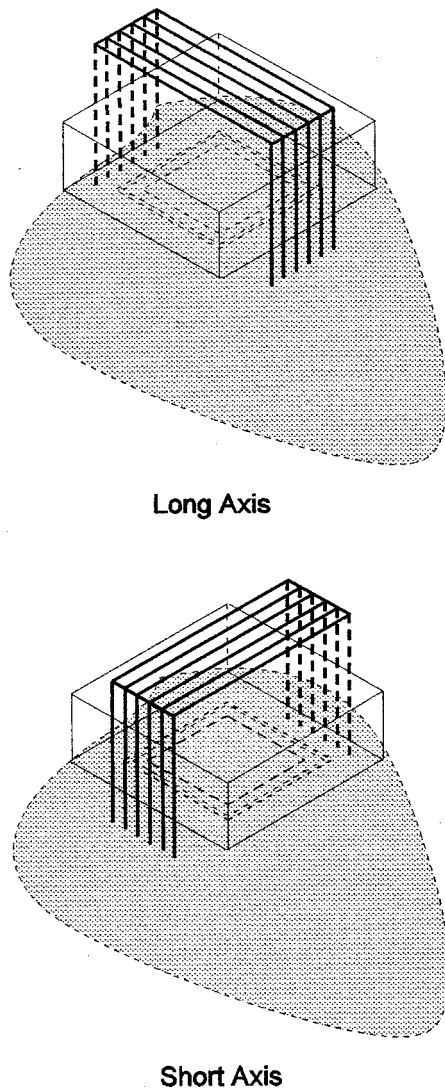


Fig. 4 Image planes for MR tagging. In order to acquire a three-dimensional deformation field, five image sequences were obtained in two orthogonal directions with image planes parallel to the walls of the suction cup. Image planes are approximately aligned with the long and short axes of the heart.

[14]. Sets of magnetically tagged planes are created immediately after a trigger. MR images orthogonal to both tagged planes are then acquired at different time delays after the trigger during the pump cycle. On the image plane, the magnetically tagged planes appear as tag lines and their intersections as tag intersection points. As epicardial suction is applied, the heart wall deforms and images acquired at later time delays show the deformed location of the tag intersection points. These points are used to measure displacements at numerous locations.

Imaging was performed using a whole body 1.5 Tesla scanner (Magnetom Vision, Siemens Medical Systems, Iselin, NJ). The fixture holding the suction cup incorporated a small circular “orbit” coil (21 cm OD, 13 cm ID, 2.4 cm thick, Siemens) to read the MR signal. The orbit coil was close to the heart and thus provided an adequate signal-to-noise ratio for high spatial resolution images. Image planes were selected parallel to the sides of the suction cup (Fig. 4). Five image planes were selected in each direction, with one slice passing through the center of the suction cup and additional slices offset by 3 and 6 mm on either side. The double DANTE RF pulses created tag lines with 3.0 mm center-to-center spacing. During each pump cycle, a synchronization

pulse was input to a trigger circuit [15], which initiated the imaging sequence. Twelve time frames were acquired at 15 ms intervals during each pump cycle. The maximum acquisition time for all tagged image sequences at a site was 43 minutes, although this was reduced to 22 minutes in experiments 06–08. The pump was then turned off and additional images were acquired to document the location of the suction cup with reference to the LV geometry. This procedure was repeated at up to two additional sites, typically on the LV free wall close to the apex and on the anterior wall of the LV at midventricle.

MR Image Analysis. The MR tagged images provided a reference configuration and multiple deformed configurations for each image plane. Three deformed configurations were analyzed for each experiment. These configurations corresponded to applied suction pressures in the range 0.79–3.58 kPa. Images at pressures below 0.75 kPa were not analyzed because the displacement magnitudes were small and the deformed tag point locations could not be consistently identified. For each image plane, coordinates of the intersection points on the reference and the deformed configurations were analyzed using a custom software package [15]. These locations were used to determine the displacement in the plane of the image at the tag intersection points for each deformed configuration and each image plane.

FE Model. A detailed description of the FE method we used is given in Costa et al. [16]. The Galerkin FE equations for three-dimensional finite elasticity (virtual work formulation) were derived in prolate spheroidal coordinates, allowing the ventricular geometry and boundary conditions to be modeled with fewer low-order elements. A three-dimensional solid mathematical representation of the LV was developed for each experiment from MR images of the heart. This process has been previously described in detail [17]. Briefly, the model geometry was subdivided so that FE nodes corresponded to the locations of the edges and corners of the suction cup. Each model had a total of 500 nodes and 360 isoparametric finite elements with trilinear Lagrange basis functions for each of the prolate spheroidal coordinates. Nodes on the epicardium at the edges of the suction cup were fully constrained. The epicardial element surfaces within the suction cup boundaries were loaded with the experimentally measured pressure for each deformed configuration.

Constitutive Relation. Although this method can be applied with many types of constitutive relation, for this analysis we modeled the ventricular wall as pseudoelastic and having an exponential strain energy function. The wall was modeled as either a homogeneous, exponential, transversely isotropic material, or as an exponential, transversely isotropic myocardium covered by a thin, isotropic epicardium. The material anisotropy of the ventricular wall was defined by referring the stress tensor components at every point in the element to an orthogonal system of local material coordinates, having one axis aligned with the fiber direction. Following the approach in Guccione et al. [11], the passive, intact ventricular wall was modeled using a strain energy potential W that was an exponential function of Lagrangian strain tensor components E_{ij} referred to fiber coordinates in the undeformed body:

$$W = \frac{C}{2} (e^Q - 1)$$

where

$$Q = b_f E_{ff}^2 + b_t (E_{cc}^2 + E_{rr}^2 + E_{cr}^2 + E_{rc}^2) + b_{fs} (E_{fc}^2 + E_{cf}^2 + E_{fr}^2 + E_{rf}^2) \quad (1)$$

and E_{ff} is fiber strain, E_{cc} is cross-fiber in-plane strain, E_{rr} is radial strain, E_{cr} is shear strain in the cross-fiber–radial coordinate plane, and E_{fc} and E_{fr} are shear strains in the fiber–cross-fiber and fiber–radial coordinate planes, respectively. The constant C scales all the stress components and the constants b_f , b_t , and b_{fs} multiply the strain terms in the exponent. The form for the

exponent Q describes the special case of three-dimensional transverse isotropy with respect to the fiber coordinate system. The fiber orientation field was described in the model by assuming that fibers lie in circumferential and longitudinal FE coordinate planes, which form the endocardial and epicardial surfaces. The orientation of fibers with respect to the circumferential direction was interpolated for each FE model geometry using fitted data from a canine heart [2]. The stress-free reference state was assumed to be at zero suction pressure with the suction cup attached. When the heart wall was modeled as having a separate epicardium, the myocardium was modeled using Eq. (1), and the constitutive relation for the epicardium was assumed to have the same form, but with all exponential coefficients set equal, which describes an isotropic material.

Model Solution. The nonlinear system of equations was solved for the unknown nodal displacements and hydrostatic pressure parameters at each incrementally increasing load step using Newton iteration. Nodal displacement solutions were written out at each experimental pressure value for use in the material parameter optimization. We compared the displacement of all data points that fell within the central region elements (three circumferential by three radial by four transmural) with FE model predictions. Data points outside the suction cup region were not used because the experimentally measured displacements were very small, and the FE model predictions were expected to be less accurate close to the edges of the suction cup, since rigid displacement constraints were imposed on the epicardium along those edges. Adding elements close to the cup boundary would also increase the computation time of each iteration of the optimization procedure, which was already computationally intensive. We ran numerous meshes with increasing numbers of elements and determined that the 360-element mesh provided good convergence (i.e., adding more elements changed the solution in the central portion of the cup very little). The model-predicted three-dimensional displacement of each data point was calculated using an inverse mapping. The MR tagging technique only measures displacement within the plane of the image, however. Thus, the component of the three-dimensional displacement vector normal to the image plane was subtracted from the displacement so that:

$$\mathbf{u}_i = \mathbf{u}_i^{\text{FE}} - (\mathbf{u}_i^{\text{FE}} \cdot \mathbf{n}) \mathbf{n} \quad (2)$$

where \mathbf{u}_i^{FE} is the model predicted three-dimensional displacement vector at experimental data point i , \mathbf{u}_i is the model predicted in-plane displacement vector, and \mathbf{n} is the normal vector of the image, all expressed in cardiac Cartesian coordinates.

Material Parameter Optimization. We followed an approach similar to that of Moulton et al. [18] to determine regional myocardial material properties from an FE model and a set of MR tagged image data. However, we formulated our objective function with respect to measured displacements rather than strain and chose a different formulation for the constitutive relation. We minimized the sum of the squared differences between the FE model predicted and experimental in-plane displacement components measured at three suction pressures. Thus the form for our objective function, S , was:

$$S(\mathbf{b}) = \sum_{i=1}^m \sum_{j=1}^3 (\hat{u}_{ij} - u_{ij})^2 \quad (3)$$

where \hat{u}_{ij} is the j th component of the measured displacement at the i th data point, u_{ij} is the j th component of the FE model in-plane displacement at the i th data point, m is the number of measurements and $\mathbf{b} = \{C, b_f, b_t, b_{fs}\}^T$ is the vector of four unknown material parameters.

This nonlinear least-squares optimization was performed using a Levenberg-Marquardt algorithm, following Moulton et al. [18]. The FE model was solved using an initial estimate for the material parameters from Guccione et al. [11] and the solution used to

calculate the value of the objective function. Finite difference approximations to the partial derivatives of the objective function with respect to each material parameter were obtained by increasing one material parameter by five or ten percent, re-solving the forward FE solution, and calculating the approximate partial derivative for that parameter. The parameter values for the next iteration, $\mathbf{b}^{(k+1)}$, were determined from:

$$\mathbf{b}^{(k+1)} = \mathbf{b}^{(k)} - (\mathbf{J}^{(k)T} \mathbf{J}^{(k)} + \Lambda \mathbf{I})^{-1} (\mathbf{J}^{(k)} \cdot \mathbf{r}^{(k)}) \quad (4)$$

where $\mathbf{J}^{(k)}$ is the Jacobian matrix, $\mathbf{r}^{(k)}$ is the residual vector, and $\mathbf{b}^{(k)}$ is the material parameter vector at the k th iteration and Λ is a scalar multiplying the identity matrix \mathbf{I} . At each iteration, a new forward FE solution and partial derivative matrix was calculated. Iteration continued until the value of the objective function S decreased by less than 0.2 percent between two consecutive iterations. For the homogeneous model of the heart wall, four parameters were optimized simultaneously. When the heart wall was modeled with a separate epicardium, two additional parameters were also optimized: C_{epi} and b_{epi} . These correspond to the scaling parameter and the single exponential parameter.

Each iteration of the optimization process for the homogeneous model of the heart wall required approximately 2.5 hours running on SGI Challenge server (Silicon Graphics Inc., Mountainview, CA) with 1.024 Gbyte of main memory. The model with separate epicardium required approximately six hours per iteration. This was due to the additional FE solutions required to calculate the Jacobian as well as an increased time to obtain each FE solution.

FE Model of Passive Inflation. In order to test how well the optimized parameters could predict experimental results obtained under different loading conditions, we used the optimized material parameters for both models of the heart wall in an FE model of passive LV filling [11] to predict transmural strain and stress distributions at an LV cavity pressure of 1 kPa. The FE geometry was axisymmetric, but the FE model was fully three-dimensional, allowing prediction of all six Lagrangian strain components. The initial axisymmetric geometry had 14 elements in the longitudinal direction and was refined into four elements transmurally, each 25 percent of the wall thickness, to obtain converged solutions using the optimized material parameters for the homogeneous model of the heart wall. To model the thin epicardium, the outermost elements were again subdivided transmurally, so that the epicardial elements were 2.5 percent of the wall thickness, the same percentage used in the models of epicardial suction.

Results

The suction pressures applied to the heart varied between 0 and 4.4 kPa (33 mmHg) during each 500 ms pump cycle. The magnitude of the suction pressure increased during a 150–200 ms period in each cycle, and images were acquired every 15 ms during this period. The pressure waveform was very repeatable from cycle to cycle. While there was some variation in peak suction pressure from experiment to experiment, these variations were accounted for by loading the FE model with the measured suction pressures for each experiment.

The complex deformation caused by the epicardial suction can be seen in short and long axis MR tagged images (Fig. 5). At the center of the suction cup, the heart wall undergoes a bending deformation. This can be seen by the radial thickening with circumferential and longitudinal compression near the endocardium and radial thinning with circumferential and longitudinal stretching near the epicardium. Away from the center of the suction cup, the initially square regions formed by adjacent tag intersection points are distorted into trapezoidal regions, which indicates significant transverse shearing. In the short axis images, circumferential–radial shearing is seen, while longitudinal–radial shearing is seen in the long axis images.

Optimized material properties were obtained for the five of the eight hearts with the suction cup placed on the lateral free wall of

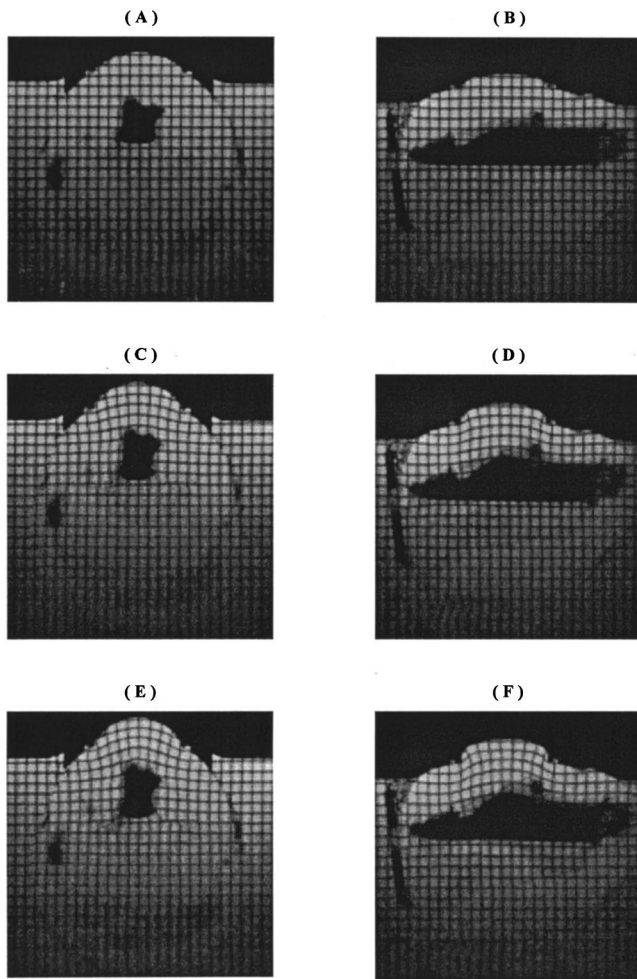


Fig. 5 MR tagged images through center of suction cup for experiment 06. (A) and (B): Undeformed short and long-axis images. (C) and (D): Images acquired at $t=60$ ms, suction pressure=2.3 kPa. (E) and (F): Images acquired at $t=105$ ms, suction pressure=3.2 kPa.

the midventricle using the homogeneous model of the heart wall (Table 1) and the model with a separate, isotropic epicardium (Table 2). The three other experiments were not analyzed due to difficulties with pressure data acquisition or due to insufficient coronary perfusion with cardioplegic solution during cardiac arrest (improper cross-clamping of aorta); the latter resulted in an essentially undeformable LV wall. The optimized material properties were obtained using displacements measured at three different suction pressures and from both long-axis and short-axis images. The mean displacement error for each experiment was computed by calculating the magnitude of the difference between FE predicted in-plane displacement and the experimentally measured displacement at each data point. Note that for all experiments, the mean displacement error is slightly less for the model with a separate, isotropic epicardium.

The deformed shape and transmural strain distributions were determined from the FE model solution with the optimized material parameters. The FE model is able to reproduce the experimental deformation pattern as shown by short and long axis deformed shape plots through the center of the suction cup for a representative experiment (Fig. 6). The transmural distributions of three-dimensional strain components referred to cardiac coordinates are shown in Figs. 7(A) and 7(B) for the center of the suction cup at a suction pressure of 3.2 kPa. Notice that longitudinal strain is negative near the endocardium and positive near the epicardium, whereas radial strain is positive near the endocardium and negative close to the epicardium. These strain patterns correspond to the bending mode of deformation evident in Fig. 5. While the shear strain components are generally small at the center of the suction cup, due to the symmetry of the loading, the transverse shears referred to cardiac coordinates are larger away from the center of the cup, as shown in Figs. 7(C) and 7(D). The largest circumferential–radial shear strain (0.12) occurs at the subendocardium in the elements anterior to the center of the suction cup (to the left as viewed from the epicardium). The maximum longitudinal–radial shear strain magnitude of 0.13 occurs at the subendocardium toward the base. The magnitudes of both shear strain components decrease toward the epicardium. The deformed shape and strain distributions (not shown) are similar for the model with separate epicardium. This is not surprising because both models fit the experimental displacement data reasonably well.

Table 1 Optimized material parameters obtained for a homogeneous, exponential, transversely isotropic model of the heart wall and the measured pressures at which experimental displacements were analyzed.

Experiment	Pressures Analyzed (kPa)	Number of Data Points	Final Values of:				Mean Disp. Error (cm)
			C	b_f	b_t	f_{fs}	
01	0.84, 2.10, 3.58	394	0.3913	75.4109	33.8617	11.4987	0.018
03	1.10, 2.04, 2.94	407	1.0173	77.4928	8.0161	3.1216	0.018
04	0.84, 2.39, 3.20	400	0.7476	39.5292	6.1735	5.6649	0.022
06	0.79, 2.31, 3.17	371	0.3047	49.8868	11.1146	14.6322	0.027
07	0.80, 1.81, 3.48	316	0.1008	93.0273	61.6131	73.1017	0.022

Table 2 Optimized material parameters obtained for a model of the heart wall, which consisted of an exponential, transversely isotropic myocardium and separate isotropic, exponential epicardium. The experimental displacements and pressures were identical to those in Table 1.

Experiment	Final Values of:						Mean Disp. Error (cm)
	C_{myo}	b_f	b_t	b_{fs}	C_{epi}	b_{epi}	
01	1.0543	31.1587	3.7345	3.6864	3.1421	44.1244	0.016
03	1.1432	70.8788	3.0269	2.0001	1.9891	25.0824	0.017
04	0.8759	13.6637	2.4250	2.9397	5.5866	15.5139	0.020
06	0.3595	53.4451	5.7746	10.1587	0.7122	21.7263	0.026
07	0.9897	10.2389	0.6979	3.7499	0.6468	95.2716	0.021

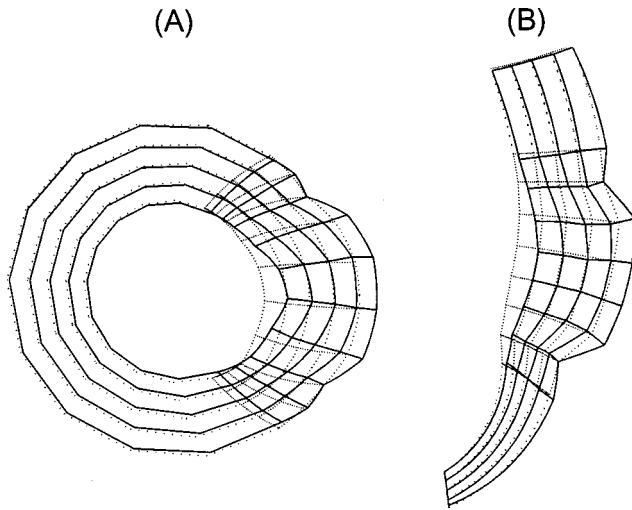


Fig. 6 Deformed shape plots of FE solution (Exp. 06) with optimized homogeneous material parameters at suction pressure of 3.2 kPa, corresponding to Figs. 5(E) and 5(F). (A) Short-axis view through center of suction cup (B) Long-axis view through center of suction cup.

In order to test whether the optimized material parameters could be used to predict deformation under a different loading, the transmural variations in strain components predicted by the axisymmetric FE model were compared to experimentally determined strain distributions [10] obtained at the midventricular region of the anterior LV free wall. The predicted strain component values are shown for both the homogeneous model of the heart wall and for the model with the separate epicardium in Fig. 8. Note that the values for each model of the heart wall are the mean values obtained from the five experiments. Thus, while both models fit the experimental data from epicardial suction well, much

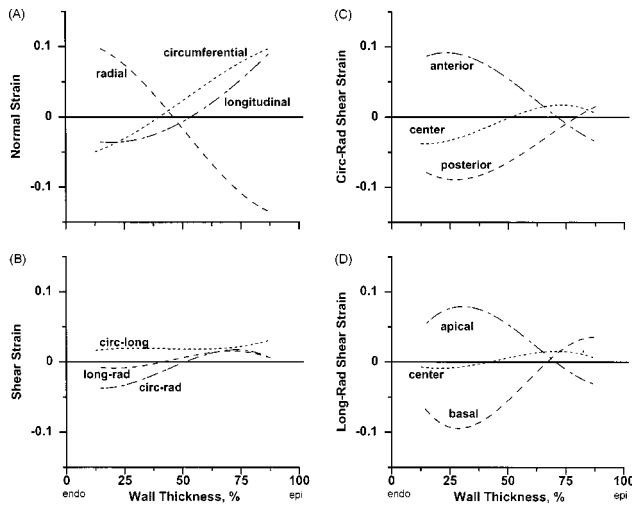


Fig. 7 Normal (A) and shear (B) strain components as a function of transmural position in FE elements through center of suction cup. (C) Radial-circumferential shear strains in elements through the center of suction cup and to the anterior and posterior of center elements. (D) Radial-longitudinal shear strains in elements through the center of suction cup, and in elements toward the apex and base. All values were predicted from the FE model for experiment 06 using optimized material parameters at experimental pressure of 3.2 kPa as shown in Fig. 6.

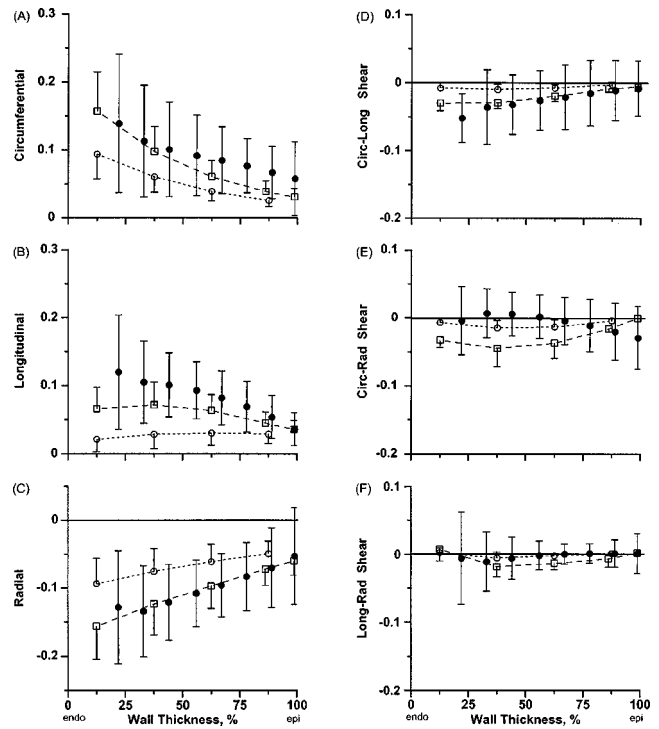


Fig. 8 Transmural variation in strain components in FE model of passive LV filling computed at 1 kPa cavity pressure. Lagrangian strain components referred to cardiac coordinates for five experiments were computed at the central gauss point of midventricular elements. Results shown are mean values with one-sided error bars of 1 SD for the model assuming homogeneous, transversely isotropic heart wall (open circles) and transversely isotropic myocardium and isotropic epicardium (open squares). Closed circles with error bars (± 1 SD) represent experimental data of Omens et al. [10] on the anterior wall of the LV at midventricle at the same cavity pressure.

closer agreement to the strain data of Omens et al. [10] is obtained when the heart wall is modeled as having a separate epicardium.

Discussion

In this study, we developed a new approach to the mechanical testing of the ventricular wall and made the first estimates of material properties for passive myocardium under significant transverse shear. This study is also the first, to our knowledge, to determine anisotropic myocardial material properties from MR tagging using a three-dimensional FE model. In agreement with previous studies [7,8,19], the myocardial material parameter values we obtained for both the homogeneous model and the model with separate epicardium demonstrated that myocardium is nonlinear and anisotropic with greater stiffness in the fiber direction. Our results also suggest that the epicardium plays a significant role in passive ventricular mechanics.

Our motivation for developing epicardial suction was to overcome the limitations of biaxial testing in determining passive material properties of the myocardium. Although biaxial testing has provided much information about the behavior of passive myocardium, such as anisotropy and nonlinearity, it is not possible to produce compressive strains or transverse shear strains and it has also been limited to a maximum of two specimens from the same heart [7]. Epicardial suction, on the other hand, creates local bending and shearing deformation of the passive heart wall. The resulting deformation is measured noninvasively with MR tagging, which allows us to obtain a dense set of displacement measurements at each suction site. By moving the suction cup to different sites on the heart wall, we can investigate behavior at different

locations in the intact heart wall. However, the process of estimating material parameters from an epicardial suction experiment is much more involved than the process of estimating material parameters from biaxial testing.

We tested whether the form of constitutive relation affected our results by optimizing material parameters for the polynomial constitutive relation proposed by Humphrey et al. [19]. We assumed the heart wall was homogeneous, and used the FE model and epicardial suction displacement data for experiment 01. The polynomial form with optimized parameters fit the epicardial suction data about as well as the exponential form. When these optimized parameters were used in the FE model of passive inflation, the magnitudes of the predicted strains were, on average, larger, with the maximum difference between strain components being 0.04. This suggests that additional experiments performed on the same heart, such as passive inflation, might allow us to distinguish between forms better. Optimized material parameters can also be obtained in an orthotropic form of the constitutive relation motivated by observations that the myocardium has a laminar structure. An orthotropic model requires a description of the local sheet orientation throughout the LV, however, and currently only limited data on sheet orientation are available [20]. Consequently, we restricted our first estimates of material properties for passive myocardium under significant transverse shear to a transversely isotropic form of constitutive relation.

Previous mathematical models of the intact LV have assumed the passive heart wall is a homogeneous material with the mechanical properties of the myocardium. However, mechanical studies of excised epicardium have shown it is a much more nonlinear material than myocardium [21–23]. Furthermore, Kang and Yin [24] performed biaxial tests on myocardial specimens with and without epicardium attached and concluded that the epicardium is stretched up to 10 percent circumferentially in the intact, unloaded rabbit LV. The values we obtained for the epicardial material parameters indicate that canine epicardium is also highly nonlinear. Moreover, when equibiaxial stretch is simulated using those material parameter values, the same stretch produces greater stresses under equibiaxial loading than those measured by Humphrey et al. [22], suggesting that the canine epicardium is also stretched in the unloaded *in vivo* state. Recently, Criscione et al. [25] suggested that the endocardium contributes to the mechanical response of papillary muscles during extension and torsion. However, since the endocardium is a thin membrane and undergoes compressive in-plane stresses during epicardial suction, we feel it would not contribute substantially to the mechanical response in this loading.

Altered coronary perfusion can change apparent diastolic stiffness of ventricular myocardium—the “garden hose” effect. For example, May-Newman et al. [26] found that myocardial strains are reduced during ventricular filling, primarily along the directions transverse to the coronary microvessels. Recently, May-Newman et al. [27] described a new mathematical model of the mechanics of perfused myocardium derived using homogenization theory. In this model, perfused myocardium is treated as a nonlinear anisotropic elastic solid embedded with cylindrical vessels of known distensibility. Since our experimental preparation is unperfused, our results reflect the mechanical behavior of this solid with unpressurized vessels.

The isolated arrested canine heart is an experimental model of normal diastolic filling, and probably is most realistic at end-diastole when relaxation of the contractile muscle fibers is most complete. The deformation induced by epicardial suction is not physiological when compared with that which occurs during normal diastolic filling, except perhaps near the epicardium, where both types of loading induce local circumferential and longitudinal stretching, radial thinning, and small transverse shear strains. However, the deformation induced by epicardial suction may be

similar to that which occurs in an ischemic or chronically infarcted ventricular region that undergoes bulging or local inflation during systolic contraction.

Potential Limitations. MR tagging is well suited to measuring the controllable and repeatable deformation caused by epicardial suction. However, errors in the measured displacements occur if the tagged image analysis program does not accurately identify the tag point intersections on the undeformed or any of the deformed configurations. We verified that the tag intersection points calculated by the semi-automated program appeared to lie close to the actual intersection points and discarded any points that appeared to be grossly in error. For experiment 02, the tagged data analysis was performed by two different investigators. Both sets of data were used independently to determine material parameters in the homogeneous model of the heart wall with other inputs to the model held constant (i.e., pressure, FE model geometry, fiber angles). The two sets of parameters were used in the simulation of passive inflation. Predicted strain components differed by less than 0.01.

A limitation of MR tagging is the lengthy data acquisition time. Using our current tagging pulse sequences, it takes approximately 22 minutes to acquire the ten sets of tagged images for each site. When the time necessary for setting up each site and acquiring geometry images was included, we were effectively limited to three sites per heart in a four hour period after arresting the heart. While decreasing the number of lines in the image and the number of signal averages reduces the image acquisition time, the spatial resolution or the signal-to-noise ratio, and hence image quality, will also be reduced. Despite this limitation, we can obtain clearer MR images with a higher tag line density than are obtained from an *in vivo* heart because we use a controlled, repeatable loading and an orbit coil. With 3 mm tag line spacing, we obtain three to four tag intersection points across the heart wall in the region of interest. In future, the spatial resolution of the images and tag line density could be increased by using a higher magnetic field gradient strength.

We were able to identify clearly the endocardial and epicardial boundaries of the heart wall and the location of the suction cup on our MR images. Although our FE model had a large number of elements, we could not include all details of the LV geometry. In particular, we chose to smooth the contours of the papillary muscles and use few elements to represent the portions of the LV wall remote from the suction cup. These simplifications were necessary to make the FE model solution tractable. We performed extensive tests on representative FE model geometry to determine the minimum number of elements required for a converged solution. We considered a converged solution as one in which the total strain energy integrated over the model and the nodal displacements did not change significantly when further degrees of freedom were added to the model [17].

We also assumed that our reference configuration for measuring displacements was a stress-free configuration. Recent studies have shown that there are residual stresses present in the LV [24,28,29]. These residual stresses could be added to our model by defining another stress-free configuration and calculating deformation gradient tensors from the stress-free configuration to the reference configuration in the manner of Guccione et al. [8]. However, this will require a full three-dimensional description of the residual stress field of the entire LV that is not yet available. The vacuum channel surrounding the suction orifice was also assumed not to effect the deformation caused by epicardial suction. A simplified FE model of the deformation caused by the vacuum channel suggested that significant deformations, and hence stresses, were confined to a local region around channel boundaries [17].

We used experimentally measured displacements rather than the experimentally derived strains [18] in our optimization objective function. The use of displacements has two benefits over strain or displacement gradient fields. Since strains are derived

from displacements, errors in displacement measurements can induce large errors in calculated experimental strains. In addition, when MRI is used to measure experimental displacements, a full three-dimensional strain field must be reconstructed from sets of orthogonal images. Several authors have presented methods for reconstructing a three-dimensional strain or displacement gradient field [30–32] over the entire LV; however, these techniques are quite complex and may require smoothing of the displacement data to avoid large local variations in the strain field. By comparing FE and experimental in-plane displacement components, we did not need to calculate an experimental three-dimensional strain prior to the optimization and thus avoided these complexities. The direct use of displacement data was simplified because epicardial suction does not impose a rigid-body motion of the entire heart as observed *in vivo*. When a rigid-body motion is present, the rigid body displacement vector must be subtracted from the experimentally measured displacement at each point prior to comparing the displacements and the FE model predictions.

The time required to optimize material parameters increases with the number of parameters being optimized. When optimizing four parameters, each iteration requires five forward FE solutions: one using the current value of the material parameters, and four to calculate the finite difference approximation to the Jacobian. For each additional optimized parameter, another FE solution is required during each iteration. Typically, the material parameter optimization converged in five to ten iterations. On the SGI Challenge server, the optimization with four material parameters required 15 to 30 hours. With increasingly powerful computers, however, these times will decrease significantly.

The optimization procedure obtains best-fit material parameters for an assumed form of constitutive relation. In our study, two forms of the myocardial constitutive relation fit our experimental data nearly as well as the model with the separate epicardium. The difference in the mean error per data point was smaller than our uncertainty in identifying the tag intersection points. Furthermore, the model with the separate epicardium had two additional material parameters that could be varied and one might thus expect a better fit to the experimental data. We concluded that the model using the separate epicardium was more appropriate because of the better fit to previous experimental data rather than based on the better fit to our epicardial suction data. Clearly it would be preferable to obtain data for both types of loading on the same hearts in future experiments.

Previously, Young et al. [33] validated MR tagging as a method to estimate material deformation using a deformable silicone gel phantom in the shape of a cylindrical annulus. Thus, use of this or a similar material in the form of a thick-walled balloon could provide additional validation of our overall technique. However, the mechanical properties of the passive ventricular wall are significantly more complex than those of an isotropic silicon gel phantom. Costa et al. [16] validated our three-dimensional FE method using analytical solutions for anisotropic solids undergoing large elastic deformations. Importantly, in each of our five experiments, we obtained parameter values for constitutive relations for the passive ventricular wall that allowed our validated FE method to reproduce the deformation measured with MRI tagging accurately. Moreover, we tested the predictive capability of these relations against myocardial deformation measured under completely different loading conditions (physiological LV filling) with another validated method (biplane X-ray of implanted markers).

Future Applications. While it would be desirable to perform epicardial suction *in vivo*, there would also be additional technical challenges. Foremost, it would be difficult to synchronize the epicardial suction pump cycle with the diastolic filling phase of the cardiac cycle. The corresponding FE analysis would also become more complicated because of the nonzero ventricular chamber and coronary artery perfusion pressures, as well as the significant myocardial deformation away from the region of interest.

Epicardial suction should also be appropriate for mechanical

testing of the passive right ventricular (RV) wall. Additional limitations for this purpose include: (1) approximately one-third as many MR tags across the RV wall; and (2) more “irregular” curvature of its epicardial surface, which would complicate the machining of a suction cup. In contrast, the atria are so thin that biaxial testing probably would be more appropriate than epicardial suction.

Conclusions

Numerous studies have sought to determine the appropriate form for three-dimensional constitutive relations for passive myocardium and associated parameter values. These studies have tested either isolated myocardial tissue under uniaxial and biaxial loading or physiological loading of the intact heart wall using passive inflation of the LV. Epicardial suction is a novel non-physiological loading technique that creates compressive and shear strains in the heart wall that can be measured by MR tagging. This method, when coupled with a full three-dimensional nonlinear FE model, provides a new way to obtain parameters for three-dimensional constitutive relations of the intact LV wall. In the material parameter optimization process, the form of the constitutive relation is assumed *a priori*. As our results demonstrate, it is not always possible to distinguish which form of the constitutive relation or model of the heart wall is most appropriate solely from epicardial suction experiments. Thus, epicardial suction should prove most useful when used in conjunction with other experimental techniques to determine material properties.

Acknowledgments

This work was supported by a grant from The Whitaker Foundation (J. M. Guccione). This support is gratefully acknowledged. The authors thank Felix Ungacta and Donna Marquardt for their assistance with the animal preparation, and Peter Hunter and Andrew McCulloch for providing the CMISS FE program.

References

- [1] Lew, W. Y. W., 1987, “Influence of Ischemic Zone Size on Nonischemic Area Function in the Canine Left Ventricle,” *Am. J. Physiol.*, **252**, pp. H990–H997.
- [2] Nielsen, P. M. F., Le Grice, I. J., Smaill, B. H., and Hunter, P. J., 1991, “Mathematical Model of Geometry and Fibrous Structure of the Heart,” *Am. J. Physiol.*, **260**, pp. H1365–H1378.
- [3] Costa, K. D., Hunter, P. J., Wayne, J. S., Waldman, L. K., Guccione, J. M., and McCulloch, A. D., 1996, “A Three-Dimensional Finite Element Method for Large Elastic Deformations of Ventricular Myocardium: II—Prolate Spheroidal Coordinates,” *ASME J. Biomech. Eng.*, **118**, pp. 464–472.
- [4] Demer, L. L., and Yin, F. C. P., 1983, “Passive Biaxial Mechanical Properties of Isolated Canine Myocardium,” *J. Physiol. (London)*, **339**, pp. 615–630.
- [5] Yin, F. C. P., Strumpf, R. K., Chew, P. H., and Zeger, S. L., 1987, “Quantification of the Mechanical Properties of Noncontracting Canine Myocardium Under Simultaneous Biaxial Loading,” *J. Biomech.*, **20**, pp. 577–589.
- [6] Smaill, B. H., and Hunter, P. J., 1991, “Structure and Function of the Diastolic Heart: Material Properties of Passive Myocardium,” in: *Theory of Heart: Biomechanics, Biophysics, and Nonlinear Dynamics of Cardiac Function*, L. Glass, P. J. Hunter, and A. D. McCulloch, eds., Springer-Verlag, New York, pp. 1–29.
- [7] Novak, V. P., Yin, F. C. P., and Humphrey, J. D., 1994, “Regional Mechanical Properties of Passive Myocardium,” *J. Biomech.*, **27**, pp. 403–412.
- [8] Guccione, J. M., McCulloch, A. D., and Waldman, L. K., 1991, “Passive Material Properties of Intact Ventricular Myocardium Determined From a Cylindrical Model,” *ASME J. Biomech. Eng.*, **113**, pp. 42–55.
- [9] Omens, J. H., MacKenna, D. A., and McCulloch, A. D., 1993, “Measurement of Strain and Analysis of Stress in Resting Rat Left Ventricular Myocardium,” *J. Biomech.*, **26**, pp. 665–676.
- [10] Omens, J. H., May, K. D., and McCulloch, A. D., 1991, “Transmural Distribution of Three-Dimensional Strain in the Isolated Arrested Canine Left Ventricle,” *Am. J. Physiol.*, **261**, pp. H918–H928.
- [11] Guccione, J. M., Costa, K. D., and McCulloch, A. D., 1995, “Finite Element Stress Analysis of Left Ventricular Mechanics in the Beating Dog Heart,” *J. Biomech.*, **28**, pp. 1167–1177.
- [12] Waldman, L. K., Fung, Y. C., and Covell, J. W., 1985, “Transmural Myocardial Deformation in the Canine Left Ventricle: Normal *In Vivo* Three-Dimensional Finite Strains,” *Circ. Res.*, **57**, pp. 152–163.
- [13] Wicomb, W. N., and Cooper, D. K. C., 1990, “Storage of the Donor Heart,” in: *The Transplantation and Replacement of Thoracic Organs*, Cooper, D. K. C., and Novitsky, D., eds., Kluwer Academic, Boston, pp. 51–61.
- [14] Mosher, T. B., and Smith, M. B., 1990, “A DANTE Tagging Sequence for the

- Evaluation of Translational Sample Motion," *Magn. Reson. Med.*, **15**, pp. 334–339.
- [15] Creswell, L. L., Moulton, M. J., Wyers, S. G., Pirolo, J. S., Fishman, D. S., Perman, W. H., Myers, K. W., Actis, R. L., Vannier, M. W., Szabo, B. A., and Pasque, M. K., 1994, "An Experimental Method for Evaluating Constitutive Models of Myocardium in In-Vivo Hearts," *Am. J. Physiol.*, **267**, pp. H853–H863.
- [16] Costa, K. D., Hunter, P. J., Rogers, J. R., Guccione, J. M., Waldman, L. K., and McCulloch, A. D., 1996, "A Three-Dimensional Finite Element Method for Large Elastic Deformations of Ventricular Myocardium: Part I—Cylindrical and Spherical Coordinates," *ASME J. Biomech. Eng.*, **118**, pp. 452–463.
- [17] Okamoto, R. J., 1997, "Determining Mechanical Properties of Heart Muscle Using Epicardial Suction," D.Sc. thesis, Washington University, St. Louis, MO.
- [18] Moulton, M. J., Creswell, L. L., Actis, R. L., Myers, K. W., Vannier, M. W., Szabo, B. A., and Pasque, M. K., 1995, "An Inverse Approach to Determining Myocardial Material Properties," *J. Biomech.*, **28**, pp. 935–948.
- [19] Humphrey, J. D., Strumpf, R. K., and Yin, F. C. P., 1990, "Determination of a Constitutive Relation for Passive Myocardium: II. Parameter Estimation," *ASME J. Biomech. Eng.*, **112**, pp. 340–346.
- [20] Le Grice, I. L., Smaill, B. H., Chai, L. Z., Edgar, S. G., Gavin, J. B., and Hunter, P. J., 1995, "Laminar Structure of the Heart: Ventricular Myocyte Arrangement and Connective Tissue Architecture in the Dog," *Am. J. Physiol.*, **269**, pp. H571–H582.
- [21] Kang, T., Humphrey, J. D., and Yin, F. C. P., 1996, "Comparison of Biaxial Mechanical Properties of Excised Endocardium and Epicardium," *Am. J. Physiol.*, **270**, pp. H2169–H2176.
- [22] Humphrey, J. D., Strumpf, R. K., and Yin, F. C. P., 1990, "Biaxial Mechanical Behavior of Excised Ventricular Epicardium," *Am. J. Physiol.*, **259**, pp. H101–H108.
- [23] Humphrey, J. D., Strumpf, R. K., and Yin, F. C. P., 1992, "A Constitutive Theory for Biomembranes: Application to Epicardial Mechanics," *ASME J. Biomech. Eng.*, **114**, pp. 461–466.
- [24] Kang, T., and Yin, F. C. P., 1996, "The Need to Account for Residual Strains and Composite Nature of Heart Wall in Mechanical Analyses," *Am. J. Physiol.*, **271**, pp. H947–H961.
- [25] Criscione, J. C., Lorenzen-Schmidt, I., Humphrey, J. D., and Hunter, W. C., 1999, "Mechanical Contribution of Endocardium During Finite Extension and Torsion Experiments on Papillary Muscles," *Ann. Biomed. Eng.*, **27**, pp. 123–130.
- [26] May-Newman, K., Omens, J. H., Pavelec, R. S., and McCulloch, A. D., 1994, "Three-Dimensional Transmural Mechanical Interaction Between the Coronary Vasculature and Passive Myocardium in the Dog," *Circ. Res.*, **74**, pp. 1166–1178.
- [27] May-Newman, K., and McCulloch, A. D., 1998, "Homogenization Modeling for the Mechanics of Perfused Myocardium," *Prog. Biophys. Mol. Biol.*, **69**, pp. 463–481.
- [28] Omens, J. H., and Fung, Y. C., 1990, "Residual Strain in Rat Left Ventricle," *Circ. Res.*, **66**, pp. 37–45.
- [29] Costa, K. D., May-Newman, K., Farr, D., O'Dell, W. G., McCulloch, A. D., and Omens, J. H., 1997, "Three-Dimensional Residual Strain in Midanterior Canine Left Ventricle," *Am. J. Physiol.*, **273**, pp. H1968–1976.
- [30] Young, A. A., 1991, "Epicardial Deformation From Coronary Cineangiograms," in: *Theory of Heart: Biomechanics, Biophysics, and Nonlinear Dynamics of Cardiac Function*, Glass, L., Hunter, J. P., and McCulloch, A. D., eds., Springer-Verlag, New York, pp. 175–207.
- [31] O'Dell, W. G., Moore, C. C., Hunter, W. C., Zerhouni, E. A., and McVeigh, E. R., 1995, "Three-Dimensional Myocardial Deformations: Calculation With Displacement Field Fitting to Tagged MR Images," *Radiology*, **195**, pp. 829–835.
- [32] Moulton, M. J., Creswell, L. L., Downing, S. W., Actis, R. L., Szabo, B. A., Vannier, M. W., and Pasque, M. K., 1996, "Spline Surface Interpolation for Calculated 3-D Ventricular Strains From MRI Tissue Tagging," *Am. J. Physiol.*, **270**, pp. H281–H297.
- [33] Young, A. A., Axel, L., Dougherty, L., Bogen, D. K., and Parenteau, C. S., 1993, "Validation of Tagging With MR Imaging to Estimate Material Deformation," *Radiology*, **188**, pp. 101–108.